Al-Khwarizmi Engineering Journal, Vol. 10, No. 3, P.P. 78- 94 (2014)

Al-Khwarizmi Engineering Journal

Numerical Investigation of Transient Heat Conduction through a Thermal Insulation of Temperature Dependant Thermal Properties

Mishaal Abdulameer Abdulkareem

Department of Mechanical Engineering /College of Engineering /AL-Mustansiriyah University

E-mail: dr.mishal04@gmail.com

(Received 13 February 2014; accepted 8 September 2014)

Abstract

The two-dimensional transient heat conduction through a thermal insulation of temperature dependent thermal properties is investigated numerically using the FVM. It is assumed that this insulating material is initially at a uniform temperature. Then, it is suddenly subjected at its inner surface with a step change in temperature and subjected at its outer surface with a natural convection boundary condition associated with a periodic change in ambient temperature and heat flux of solar radiation. Two thermal insulation materials were selected. The fully implicit time scheme is selected to represent the time discretization. The arithmetic mean thermal conductivity is chosen to be the value of the approximated thermal conductivity at the interface between adjacent control volumes. A temperature dependent specific heat capacity proposed by a 4^{th} Degree polynomial is fitted. A good agreement is obtained when the predicted results are compared with those obtained from the analytical solution.

Keywords: *Perlite, Finite Volume, numerical, implicit, conductivity.*

1. Introduction

The performance of air separation plants and storage tanks for cryogenic liquids and liquefied hydrocarbons depends majorly on the characteristics of its thermal insulating materials. Most of these thermal insulations operate under atmospheric or medium vacuum pressure and it use Perlite (a loose granulated material of volcanic glass origin heated at 850-900 C^o to vaporize the high water content that is trapped in its structure and allowing its volume to be porous and expanded up to $7-16$ times its original volume). A common property of all cryogenic thermal insulating materials is that it operates under high temperature deference between atmospheric air and cryogenic fluid temperatures. Therefore, filling it inside a vacuumed leak tight annular space separating the atmosphere from cryogenic fluid vessels is necessary to avoid the drop in its efficiency due to the penetration and freeze of water vapor and carbon dioxide.

The sudden filling of an empty cryogenic liquid storage tank initially at atmospheric temperature with a cryogenic liquid at its saturation temperature will initiate a sudden high temperature difference between the terminals of the annular space containing the thermal insulating material. This high temperature difference is behind the dependence of thermal conductivity and specific heat capacity of the thermal insulation material on its temperature. In addition, it will initiate a potential for the evaporation of cryogenic liquid due to the transient heat transfer inside the cryogenic liquid storage tank. This energy loss is of a great economic interest especially when the size of cryogenic liquid storage tank is relatively big.

Reference [1] presented an analytical double-series solution for transient heat conduction in

polar coordinates (2-D cylindrical) for multi-layer domain in the radial direction with spatially non-uniform but time-independent volumetric heat sources. Inhomogeneous boundary conditions of the third kind are applied in the direction perpendicular to the layers. Only homogeneous boundary conditions of the first or second kind are applicable on θ = constant surfaces.

Reference [2] have used the PAK-T software package, which is based on the finite element method using the Galerkin approach to solve the non-linear transient two-dimensional heat conduction through an insulation wall of tank for transportation of liquid aluminum. The objective was to optimize, under certain boundary conditions, the thickness of the insulation material which its thermal properties is a temperature dependent.

Reference [3] presented an analytical series solution for transient boundary-value problem of heat conduction in $r-\theta$ spherical coordinates. The proposed solution is applicable in spherical cone, hemisphere, spherical wedge or full sphere. Spatially non-uniform, (only $r\,and\,\theta$-dependent), time independent volumetric heat sources may be present in the layers. Inhomogeneous, time independent, θ-dependent boundary conditions of the first, second or third kind may be applied on the inner and outer radial boundaries, and only homogenous boundary conditions of the first or second kind may be applied on the θ-direction boundary surfaces.

Reference [4] has investigated analytically the unsteady heat conduction in composite fiber winded cylindrical shape laminates. This solution is valid for the most generalized boundary conditions that combine the effects of conduction, convection and radiation both inside and outside the cylindrical composite laminates. The Laplace transformation has been used to change the problem domain from time into frequency. An appropriate Fourier transformation has been derived using the Sturm-Liouville theorem. Due to the difficulty of applying the inverse Laplace transformation, the Meromorphic function method is utilized to find the transient temperature distribution in laminate.

Reference [5] has used the cylindrical coordinates and Reference [6] has used the spherical coordinates. Both references has used the Kirchhoff's transformation to solve analytically the non-linear partial differential equation of transient heat conduction through a hollow cylindrical or spherical thermal insulation material of a thermal conductivity temperature dependent property proposed by an available empirical function. It is assumed that this insulating material is initially at a uniform temperature. Then, it is suddenly subjected at its inner radius with a step change in temperature. Four thermal insulation materials were selected. An identical analytical solution was achieved when comparing the results of temperature distribution with available analytical solution for the same four case studies that assume a constant thermal conductivity. It is found that the characteristics of the thermal insulation material and the pressure value between its particles have a major effect on the rate of heat transfer and temperature profile.

In this paper, the two-dimensional, body-fitted coordinate, non-linear partial differential equation of transient heat conduction through a thermal insulation material of a thermal conductivity temperature dependent property proposed by an available empirical function $\left(k = a + bT^c\right)$, [7], and of a temperature dependent specific heat capacity property proposed by a 4th Degree polynomial fit will be investigated numerically using the FVM. This insulating material is initially at a uniform temperature $\left(T_i\right)$. Then, it is suddenly subjected at its inner surface with a constant temperature $\left(T_o\right), \left(T_o < T_i\right)$ and subjected at its outer surface with a natural convection heat transfer boundary condition associated with a periodic change in ambient temperature $\left(T_\infty\right)$ and heat flux of solar radiation. Two thermal insulation materials will be selected, [7], each of outside radius of $\left(1m\right)$. The first is Perlite of thickness $\left(800mm\right)$ with a characteristic mean particle diameter of $\left(d_m = 0.5mm\right)$ and density of $\left(\rho = 64kg/m^3\right)$ at $\left(10^5\ Pa\right)$ atmospheric pressure. The second is Perlite of thickness $\left(200mm\right)$ with a characteristic mean particle diameter of $\left(d_m = 0.5mm\right)$ and density of $\left(\rho = 50kg/m^3\right)$ at a gas pressure $\left(\le 0.1Pa\right)$. The fully implicit time scheme will be selected to represent the time discretization. The arithmetic mean thermal conductivity will be chosen to be the value of the approximated thermal conductivity at the interface between adjacent control volumes. To validate the predicted one-dimensional results, both profiles of the temperature and the rate of heat transfer will be compared with the one-dimensional analytical close form solution, [5], which assumes that only the thermal conductivity of thermal insulation material is a temperature dependant property.

2. Finite Volume Model

2.1. Grid Generation

In the Finite Volume Method, the first step is to divide the domain into a number of discrete control volumes; (N_r) for One-Dimensional domain and $(N_r N_z)$ for Two-Dimensional domain. A general nodal point is identified by P. In One-Dimensional domain, the nodes to the west and east of P are identified by W and E respectively. The west side boundary of the control volume is referred to by 'w' and the east side of the control volume is referred by 'e', Figure (1). In Two-Dimensional domain, the nodes to the west, east, bottom and top of P are identified by W, E, B and Top respectively. The side boundaries of the control volume is referred to by; 'w', 'e', 'b' and 'top' for the west, east, bottom and top sides respectively, Figure (2). The time domain is divided into a number of time steps of size Δt. Variables at the previous time level are indicated by the superscript (o, Old). In contrast, the variables at the new time level are not superscripted [8].

2.2. Initial and Boundary Conditions of 1-D Model

Consider a hollow cylindrical thermal insulation material of temperature dependent thermal conductivity proposed by an available empirical function $\left(k = a + bT^c\right)$, [7], and of a temperature dependent specific heat capacity property proposed by a 4th Degree polynomial fit and of inside radius (R_1), outside radius $(R_2 = 1m)$ and of infinitesimal thickness Δz. This insulating material is initially at a uniform temperature $(T_i = 300K)$. The boundary condition at $(r = R_1)$ is suddenly subjected with a constant temperature $(T_o = 77K)$ while it is kept at the value of the initial temperature at $(R_2 = 1m)$. No convection or radiation heat transfer at the boundaries and no internal heat generation, as shown in Figure (3).

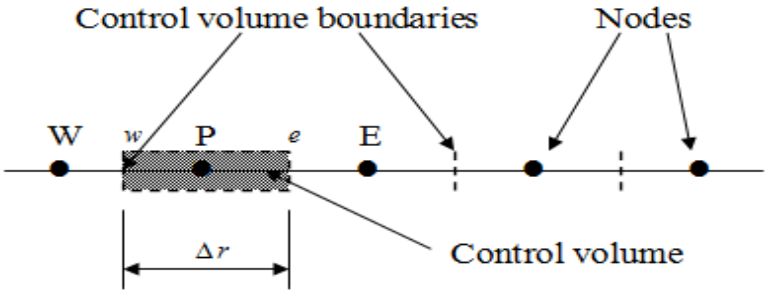

Fig. 1. One-Dimensional control volume.

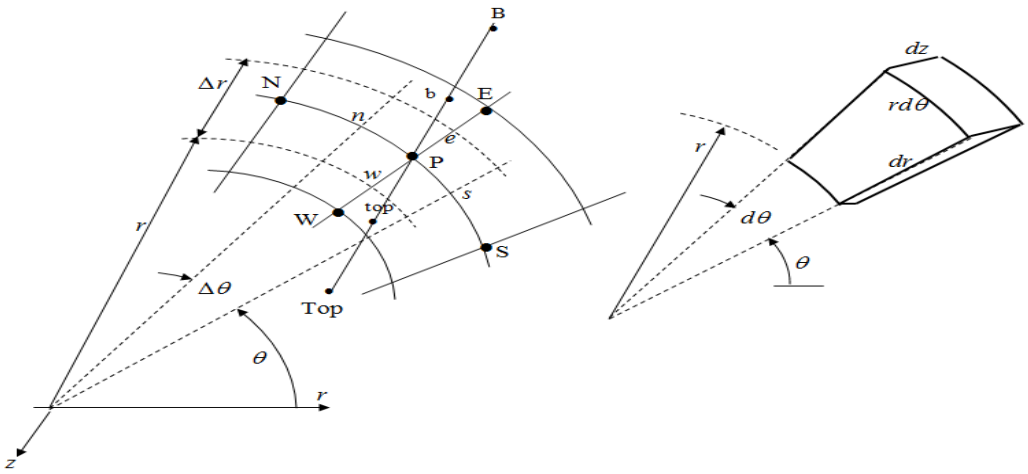

Fig. 2. Two-Dimensional control volume.

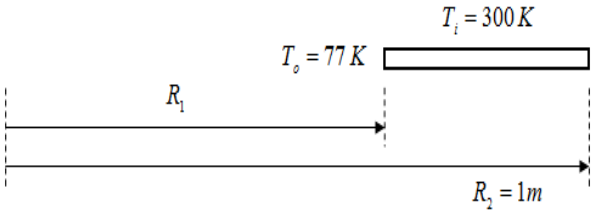

Fig. 3. Initial and boundary conditions of one-dimensional model.

(1) *Perlite in air*, $\left(R_1 = 0.2\,m, d_m = 0.5\,mm, \rho = 64\,kg/m^3\right)$.

(2) *Perlite – vacuum*, $\left(R_1 = 0.8\,m, d_m = 0.5\,mm, \rho = 50\,kg/m^3\right)$.

2.3. Discretization of 1-D model

The governing One-Dimensional energy equation is:

$$\rho C(T)\frac{\partial T}{\partial t} = \frac{1}{r}\frac{\partial}{\partial r}\left(rk(T)\frac{\partial T}{\partial r}\right), R_1 \le r \le R_2 \qquad ...(1)$$

Multiply Equation (1) by $(dV.dt)$, $(dV = r.d\theta.dr.dz)$ and then integrate over the control volume faces, yields;

$$\int_t^{t+\Delta t}\int_w^e\int_s^n\int_b^{top}(r.d\theta.dr.dz.dt)\rho C(T)\frac{\partial T}{\partial t} =$$

$$\int_t^{t+\Delta t}\int_w^e\int_s^n\int_b^{top}(r.d\theta.dr.dz.dt)\frac{1}{r}\frac{\partial}{\partial r}\left(rk(T)\frac{\partial T}{\partial r}\right)$$

Using fully implicit scheme;

$$\rho C(T) r_P\,\Delta r\left(T_P - T_P^o\right) =$$

$$\int_t^{t+\Delta t}\left[\left(r\,k(T)\frac{\partial T}{\partial r}\right)_e - \left(r\,k(T)\frac{\partial T}{\partial r}\right)_w\right]dt \qquad ...(2)$$

Each of the boundary conditions is substituted into Equation (2). Then divide each of the resulting equation by Δt and rearrange yields:

$$a_P T_P = a_E T_E + a_W T_W + a_P^o T_P^o + S_u \qquad ...(3)$$

$$a_P = a_E + a_W + a_P^o - S_P$$

$$a_P^o = \frac{\rho C(T) r_P\,\Delta r}{\Delta t}$$

Since uniform control volumes with size Δr are used. Hence, $\Delta r = (R_2 - R_1)/N_r$

Where (a_W, a_E, S_P, S_u) are listed in Table (1).

Table 1,
Discretization parameters of one dimensional model.

Zone	a_W	a_E	S_P	S_u
Internal nodes	$\frac{r_w k_w(T)}{\Delta r}$	$\frac{r_e k_e(T)}{\Delta r}$	0	0
West Boundary	0	$\frac{r_e k_e(T)}{\Delta r}$	$-\frac{r_w k_w(T)}{\Delta r/2}$	$\frac{r_w k_w(T)}{\Delta r/2} T_o$
East Boundary	$\frac{r_w k_w(T)}{\Delta r}$	0	$-\frac{r_e k_e(T)}{\Delta r/2}$	$\frac{r_e k_e(T)}{\Delta r/2} T_i$

2.4. Initial and boundary conditions of 2-D model.

Consider a Two-Dimensional model of liquid nitrogen cylindrical storage tank of a hemispherical dish head. This storage tank is covered with a hollow cylindrical thermal insulation material of temperature dependent thermal conductivity proposed by an available empirical function $\left(k = a + bT^c\right)$, [7], and of a temperature dependent specific heat capacity property proposed by a 4th Degree polynomial fit and of inside radius $\left(R_1\right)$, outside radius $\left(R_2 = 1m\right)$. This insulating material is initially at a uniform temperature $\left(T_i = 300K\right)$. The boundary condition at $\left(r = R_1\right)$ is suddenly subjected with a constant temperature $\left(T_o = 77K\right)$, as illustrated in Figure (4), and subjected at its outer surface with a natural convection heat transfer boundary condition associated with a periodic change in ambient temperature $\left(T_\infty\right)$, as shown in Figure (5), and heat flux of incident solar radiation, as show in Figure (6). The value of the free convection heat transfer coefficient between ambient air and the outer surface of the storage tank is $\left(h_o = 5\ W/m^2.K\right)$, [9], with no internal heat generation. The modeling of periodic change in ambient temperature and the transient heat flux of incident solar radiation due to movement of the sum from sunrise at (Time=6:00) to sunset at (Time=18:00) are given as follows:

$$T_\infty = T_m + \left(T_{\max} - T_m\right)\cos\left[\frac{2\pi\left(Time-12\right)}{24}\right]$$

$$T_{\max} = 300K \quad , \quad T_{\min} = 280K$$

$$and \quad T_m = \frac{T_{\max} + T_{\min}}{2} \quad , \quad Time = \frac{t}{3600} + 12$$

$$q_E = \begin{cases} 0 & , \ 0 \le Time < 6 \\ q\cos\left[\dfrac{2\pi\left(Time-6\right)}{24}\right] & , \ 6 \le Time \le 12 \\ 0 & , \ 12 < Time \le 24 \end{cases}$$

$$q_T = \begin{cases} 0 & , \ 0 \le Time < 6 \\ q\cos\left[\dfrac{2\pi\left(Time-12\right)}{24}\right] & , \ 6 \le Time \le 18 \\ 0 & , \ 18 < Time \le 24 \end{cases}$$

$$q_W = \begin{cases} 0 & , \ 0 \le Time < 12 \\ q\sin\left[\dfrac{2\pi\left(Time-12\right)}{24}\right] & , \ 12 \le Time \le 18 \\ 0 & , \ 18 < Time \le 24 \end{cases}$$

2.5. Discretization of 2-D model

The governing Two-Dimensional energy equation is:

$$\rho C(T)\frac{\partial T}{\partial t} = \frac{1}{r}\frac{\partial}{\partial r}\left(rk(T)\frac{\partial T}{\partial r}\right) + \frac{\partial}{\partial z}\left(k(T)\frac{\partial T}{\partial z}\right) \qquad \ldots(4)$$

Since the physical domain is non-uniform. Therefore, a transformation from physical domain (r, z directions) to computational domain (ξ , ζ directions) is introduced. A two dimensional body fitted coordinate system is used. The jacobian of transformation is defined as follows, [10]:

$$J = \begin{vmatrix} r_\xi & r_\zeta \\ z_\xi & z_\zeta \end{vmatrix} = r_\xi\, z_\zeta - z_\xi\, r_\zeta$$

$$where: \ r_\xi = \frac{\partial r}{\partial \xi}, \ r_\zeta = \frac{\partial r}{\partial \zeta}, \ z_\xi = \frac{\partial z}{\partial \xi}, \ z_\zeta = \frac{\partial z}{\partial \zeta}$$

Substituting the jacobian of transformation into Equation (4) and rearrange, yields:

$$J\,\rho C(T)\frac{\partial T}{\partial t} = \frac{\partial}{\partial \xi}\left(J\,a_1\,k(T)\frac{\partial T}{\partial \xi}\right) + \frac{\partial}{\partial \zeta}\left(J\,a_2\,k(T)\frac{\partial T}{\partial \zeta}\right) + \frac{\partial}{\partial \xi}\left(J\,b_1\,k(T)\frac{\partial T}{\partial \zeta}\right) + \frac{\partial}{\partial \zeta}\left(J\,b_1\,k(T)\frac{\partial T}{\partial \xi}\right) \qquad \ldots(5)$$

$$a_1 = \xi_r^2 + \xi_z^2 \quad ; \; where: \; \xi_r = \frac{\partial \xi}{\partial r} \; , \; \xi_z = \frac{\partial \xi}{\partial z}$$

$$a_2 = \zeta_r^2 + \zeta_z^2 \quad ; \; where: \; \zeta_r = \frac{\partial \zeta}{\partial r} \; , \; \zeta_z = \frac{\partial \zeta}{\partial z}$$

$$b_1 = \xi_r \, \zeta_r - \xi_z \, \zeta_z$$

Multiply Equation (5) by $(dV.dt)$, $(dV = d\xi.d\eta.d\zeta)$ and then integrate over the control volume faces, yields;

$$\int_t^{t+\Delta t} \int_w^e \int_s^n \int_b^{top} (d\xi.d\eta.d\zeta.dt) J \rho C(T) \frac{\partial T}{\partial t} =$$

$$\int_t^{t+\Delta t} \int_w^e \int_s^n \int_b^{top} (d\xi.d\eta.d\zeta.dt) \frac{\partial}{\partial \xi}\left(J \, a_1 \, k(T) \frac{\partial T}{\partial \xi} \right) +$$

$$\int_t^{t+\Delta t} \int_w^e \int_s^n \int_b^{top} (d\xi.d\eta.d\zeta.dt) \frac{\partial}{\partial \zeta}\left(J \, a_2 \, k(T) \frac{\partial T}{\partial \zeta} \right) +$$

$$\int_t^{t+\Delta t} \int_w^e \int_s^n \int_b^{top} (d\xi.d\eta.d\zeta.dt) \frac{\partial}{\partial \xi}\left(J \, b_1 \, k(T) \frac{\partial T}{\partial \zeta} \right) +$$

$$\int_t^{t+\Delta t} \int_w^e \int_s^n \int_b^{top} (d\xi.d\eta.d\zeta.dt) \frac{\partial}{\partial \zeta}\left(J \, b_1 \, k(T) \frac{\partial T}{\partial \xi} \right)$$

Using fully implicit scheme;

$$J \rho C(T) \, \Delta\xi \, \Delta\eta \, \Delta\zeta \left(T_P - T_P^o \right) =$$

$$\int_t^{t+\Delta t} \left[\left(J \, a_1 \, d\eta \, d\zeta \, k(T) \frac{\partial T}{\partial \xi} \right)_e - \left(J \, a_1 \, d\eta \, d\zeta \, k(T) \frac{\partial T}{\partial \xi} \right)_w \right] dt +$$

$$\int_t^{t+\Delta t} \left[\left(J \, a_2 \, d\xi \, d\zeta \, k(T) \frac{\partial T}{\partial \eta} \right)_n - \left(J \, a_2 \, d\xi \, d\zeta \, k(T) \frac{\partial T}{\partial \eta} \right)_s \right] dt +$$

$$\int_t^{t+\Delta t} \left[\left(J \, b_1 \, d\eta \, d\zeta \, k(T) \frac{\partial T}{\partial \eta} \right)_e - \left(J \, b_1 \, d\eta \, d\zeta \, k(T) \frac{\partial T}{\partial \eta} \right)_w \right] dt +$$

$$\int_t^{t+\Delta t} \left[\left(J \, b_1 \, d\xi \, d\zeta \, k(T) \frac{\partial T}{\partial \xi} \right)_n - \left(J \, b_1 \, d\xi \, d\zeta \, k(T) \frac{\partial T}{\partial \xi} \right)_s \right] dt \quad ...(6)$$

…(6)

Each of the boundary conditions is substituted into Equation (6). Then divide each of the resulting equation by Δt and rearrange yields:

$$a_P T_P = a_E T_E + a_W T_W + a_{Top} T_{Top} + a_B T_B + a_P^o T_P^o + S_u \quad \ldots(7)$$

$$a_P = a_E + a_W + a_{Top} + a_B + a_P^o - S_P$$

$$a_P^o = \frac{J \rho C(T) \Delta\xi \, \Delta\zeta}{\Delta t} \quad ,$$

$$\Delta\xi = \frac{1 - (R_1 / R_2)}{N_r} \; , \; \Delta\zeta = 1/N_z \; , \; \Delta\eta = 1$$

Where $(a_W, a_E, a_{Top}, a_B, S_P, S_u)$ are listed in Table (2).

2.6. Solver

Equations (3) and (7) are solved using the TDMA, [8].

3. Thermal Conductivity

The dependence of thermal conductivity on temperature is suggested by the empirical function $(k = a + bT^c)$, [7]. The values of (a, b, c) for the two selected thermal insulation materials are given in Table (3). This empirical function is valid in a temperature rang of $(77 - 400K)$.

4. Specific Heat Capacity

Each of the two selected thermal insulation materials is originally made from Quartz glass. Therefore, the temperature dependence of specific heat capacity of Quartz glass for a temperature range of $(77 - 300K)$ is given in Table (4), [11], and its relation with temperature is represented using a 4th Degree polynomial fit as shown in Table (5).

5. Results and Discussion

5.1. 1-D model

The One-Dimensional model with the chosen values of initial and boundary conditions is shown in Figure (3).

The first step to validate the numerical solution is to choose the grid and time sizes that are adequate for obtaining the minimum error of results. This task is accomplished through a Gird Independency Test GIT. Two thermal insulation materials were selected, [7]. The first is Perlite of thickness $(800mm)$ with a characteristic mean particle diameter of $(d_m = 0.5mm)$ and density of $(\rho = 64kg/m^3)$ at $(10^5\ Pa)$ atmospheric pressure, it is associated with a grid size of $N_r = 50$. The second is Perlite of thickness $(200mm)$with a characteristic mean particle diameter of $(d_m = 0.5mm)$ and density of $(\rho = 50kg/m^3)$ at a gas pressure $(\leq 0.1Pa)$ and it is associated with a grid size of $N_r = 100$. A time step of $\Delta t = 10$ min is chosen, as shown in Figure (7). The arithmetic mean thermal conductivity is chosen to be the value of the approximated thermal conductivity at the interface between adjacent control volumes, as estimated in Table (6).

Figure (8) shows a good agreement when the numerical results of temperature distribution and the rate of heat transfer, for the two selected thermal insulation materials, are compared with the analytical results at time intervals of $t = 3,6,12,18,24 and\ 72\ hr$, using a fully implicit time scheme.

Figure (8) clarify that the characteristics of the thermal insulation material and the pressure value between its particles have a major effect on the rate of heat transfer and consequently the temperature profile. For instance, the dominant heat transfer mode when choosing Perlite at $(10^5\ Pa)$ atmospheric pressure is by heat conduction of the interstitial gas between the particles, whereas the heat transfer by radiation is negligible. When the pressure within a thermal insulation material is lowered to a value, the percentage of heat transfer by heat conduction of the interstitial gas between the particles becomes negligibly small when compared with the percentage heat transfer by radiation and conduction over the bulk material. The gas pressure, at which this is reached, depends on the characteristic diameter of the thermal insulation material. A gas pressure of $(\leq 0.1Pa)$ is sufficient for Perlite with a characteristic mean particle diameter of $(d_m = 0.5mm)$.

5.2. 2-D model

The Two-Dimensional model with the chosen values of initial and boundary conditions is shown in Figures (4), (5) and (6) respectively. This Two thermal insulation materials were selected, [7]. The first is Perlite of thickness $(800mm)$ with a characteristic mean particle diameter of $(d_m = 0.5mm)$ and density of $(\rho = 64kg/m^3)$ at $(10^5\ Pa)$ atmospheric pressure. The second is Perlite of thickness $(200mm)$with a characteristic mean particle diameter of $(d_m = 0.5mm)$ and density of $(\rho = 50kg/m^3)$ at a gas pressure $(\leq 0.1Pa)$. The arithmetic mean thermal conductivity is chosen to be the value of the approximated thermal conductivity at the interface between adjacent control volumes, as estimated in Table (6). In order to obtaining the minimum error of results, a grid size of (25X200) is used to model the domain of the two selected thermal insulation materials with a time step size of $\Delta t = 10$ min, as shown in Figure (9).

Figures (10) and (11) shows the predicted numerical results of temperature distribution and the rate of heat transfer, for the two selected thermal insulation materials, at time intervals of $t = 3,6,12,18,24 and\ 45\ hr$ .The fully implicit time scheme is selected to represent the time discretization.

It is assumed that the convergence value is (0.001), which is estimated on the basis of the difference between the predicted values of temperature in two successive iterations.

Table 2,
Discretization parameters of two dimensional model.

Zone	a_E	a_W	a_{Top}	a_B	S_P	S_u
Internal nodes	$J\,\Delta\zeta\,k_e(T)\left[\frac{a_1}{\Delta\xi}+\frac{b_1}{\Delta\zeta}\right]$	$J\,\Delta\zeta\,k_w(T)\left[\frac{a_1}{\Delta\xi}+\frac{b_1}{\Delta\zeta}\right]$	$J\,\Delta\xi\,k_{top}(T)\left[\frac{a_2}{\Delta\zeta}+\frac{b_1}{\Delta\xi}\right]$	$J\,\Delta\xi\,k_b(T)\left[\frac{a_2}{\Delta\zeta}+\frac{b_1}{\Delta\xi}\right]$	0	0
Surface (BCDEFGH)	$J\,\Delta\zeta\,k_e(T)\left[\frac{a_1}{\Delta\xi}+\frac{b_1}{\Delta\zeta}\right]$	0	$J\,\Delta\xi\,k_{top}(T)\left[\frac{a_2}{\Delta\zeta}+\frac{b_1}{\Delta\xi}\right]$	$J\,\Delta\xi\,k_b(T)\left[\frac{a_2}{\Delta\zeta}+\frac{b_1}{\Delta\xi}\right]$	$-J\,\Delta\zeta\,k_w(T)\left[\frac{a_1}{\Delta\xi/2}\right]$	$J\,\Delta\zeta\,k_w(T)\left[\frac{a_1}{\Delta\xi/2}\right]T_o$
Lower Dish (JON)	0	$J\,\Delta\zeta\,k_w(T)\left[\frac{a_1}{\Delta\xi}+\frac{b_1}{\Delta\zeta}\right]$	$J\,\Delta\xi\,k_{top}(T)\left[\frac{a_2}{\Delta\zeta}+\frac{b_1}{\Delta\xi}\right]$	$J\,\Delta\xi\,k_b(T)\left[\frac{a_2}{\Delta\zeta}+\frac{b_1}{\Delta\xi}\right]$	$-J\;a_1\,\Delta\zeta\,h_o$	$J\;a_1\,\Delta\zeta\,h_o\,T_\infty$
East Surface (NM)	0	$J\,\Delta\zeta\,k_w(T)\left[\frac{a_1}{\Delta\xi}+\frac{b_1}{\Delta\zeta}\right]$	$J\,\Delta\xi\,k_{top}(T)\left[\frac{a_2}{\Delta\zeta}+\frac{b_1}{\Delta\xi}\right]$	$J\,\Delta\xi\,k_b(T)\left[\frac{a_2}{\Delta\zeta}+\frac{b_1}{\Delta\xi}\right]$	$-J\;a_1\Delta\zeta\,h_o$	$J\;a_1\Delta\zeta\left(h_o\,T_\infty+q_e\right)$
Top Dish (MLK)	0	$J\,\Delta\zeta\,k_w(T)\left[\frac{a_1}{\Delta\xi}+\frac{b_1}{\Delta\zeta}\right]$	$J\,\Delta\xi\,k_{top}(T)\left[\frac{a_2}{\Delta\zeta}+\frac{b_1}{\Delta\xi}\right]$	$J\,\Delta\xi\,k_b(T)\left[\frac{a_2}{\Delta\zeta}+\frac{b_1}{\Delta\xi}\right]$	$-J\;a_1\,\Delta\zeta\,h_o$	$J\;a_1\Delta\zeta\left(h_o\,T_\infty+q_t\right)$
West Surface (JK)	0	$J\,\Delta\zeta\,k_w(T)\left[\frac{a_1}{\Delta\xi}+\frac{b_1}{\Delta\zeta}\right]$	$J\,\Delta\xi\,k_{top}(T)\left[\frac{a_2}{\Delta\zeta}+\frac{b_1}{\Delta\xi}\right]$	$J\,\Delta\xi\,k_b(T)\left[\frac{a_2}{\Delta\zeta}+\frac{b_1}{\Delta\xi}\right]$	$-J\;a_1\Delta\zeta\,h_o$	$J\;a_1\Delta\zeta\left(h_o\,T_\infty+q_w\right)$
Face AB	$J\,\Delta\zeta\,k_e(T)\left[\frac{a_1}{\Delta\xi}+\frac{b_1}{\Delta\zeta}\right]$	$J\,\Delta\zeta\,k_w(T)\left[\frac{a_1}{\Delta\xi}+\frac{b_1}{\Delta\zeta}\right]$	$J\,\Delta\xi\,k_{top}(T)\left[\frac{a_2}{\Delta\zeta}+\frac{b_1}{\Delta\xi}\right]$	0	0	0
Face HI	$J\,\Delta\zeta\,k_e(T)\left[\frac{a_1}{\Delta\xi}+\frac{b_1}{\Delta\zeta}\right]$	$J\,\Delta\zeta\,k_w(T)\left[\frac{a_1}{\Delta\xi}+\frac{b_1}{\Delta\zeta}\right]$	0	$J\,\Delta\xi\,k_b(T)\left[\frac{a_2}{\Delta\zeta}+\frac{b_1}{\Delta\xi}\right]$	0	0
Corner A	0	$J\,\Delta\zeta\,k_w(T)\left[\frac{a_1}{\Delta\xi}+\frac{b_1}{\Delta\zeta}\right]$	$J\,\Delta\xi\,k_{top}(T)\left[\frac{a_2}{\Delta\zeta}+\frac{b_1}{\Delta\xi}\right]$	0	$-J\;a_1\,\Delta\zeta\,h_o$	$J\;a_1\,\Delta\zeta\,h_o\,T_\infty$
Corner B	$J\,\Delta\zeta\,k_e(T)\left[\frac{a_1}{\Delta\xi}+\frac{b_1}{\Delta\zeta}\right]$	0	$J\,\Delta\xi\,k_{top}(T)\left[\frac{a_2}{\Delta\zeta}+\frac{b_1}{\Delta\xi}\right]$	0	$-J\,\Delta\zeta\,k_w(T)\left[\frac{a_1}{\Delta\xi/2}\right]$	$J\,\Delta\zeta\,k_w(T)\left[\frac{a_1}{\Delta\xi/2}\right]T_o$
Corner H	$J\,\Delta\zeta\,k_e(T)\left[\frac{a_1}{\Delta\xi}+\frac{b_1}{\Delta\zeta}\right]$	0	0	$J\,\Delta\xi\,k_b(T)\left[\frac{a_2}{\Delta\zeta}+\frac{b_1}{\Delta\xi}\right]$	$-J\,\Delta\zeta\,k_w(T)\left[\frac{a_1}{\Delta\xi/2}\right]$	$J\,\Delta\zeta\,k_w(T)\left[\frac{a_1}{\Delta\xi/2}\right]T_o$
Corner I	0	$J\,\Delta\zeta\,k_w(T)\left[\frac{a_1}{\Delta\xi}+\frac{b_1}{\Delta\zeta}\right]$	0	$J\,\Delta\xi\,k_b(T)\left[\frac{a_2}{\Delta\zeta}+\frac{b_1}{\Delta\xi}\right]$	$-J\;a_1\,\Delta\zeta\,h_o$	$J\;a_1\,\Delta\zeta\,h_o\,T_\infty$

Table 3,
Empirical function for the selected thermal insulation materials, [7].

Insulating material	Empirical function $\left(k = a + bT^c\right)$, $\left(W/m.K\right)$		
	a	b	c
Perlite in air $\rho = 64 kg/m^3, d_m = 0.5 mm, p = 10^5\ Pa$	8.25×10^{-3}	1.165×10^{-4}	1.0
Perlite - vacuum $\rho = 50 kg/m^3, d_m = 0.5 mm, p \le 0.1 Pa$	1.9112×10^{-4}	3.4757×10^{-12}	3.678

Table 4,
Specific heat capacity of Quartz glass, [11].

T (K)	50	100	150	200	250	300
C (kj/kg.K)	0.095	0.21	0.41	0.54	0.65	0.745

Table 5,
Polynomial fit of specific heat capacity for Quartz glass.

$C(T) = \sum_{n=0}^{4} \beta_n T^n$, $\left(kj/kg.K\right)$

β_0	β_1	β_2	β_3	β_4
2.16667×10^{-1}	-6.485582×10^{-3}	9.92778×10^{-5}	-3.9926×10^{-7}	5.333×10^{-10}

Table (6)
Interblock nonlinear thermal conductivity.

Thermal conductivity	Arithmetic mean
$k_e(T)$	$\left[k_P(T) + k_E(T)\right]/2$
$k_w(T)$	$\left[k_P(T) + k_W(T)\right]/2$
$k_b(T)$	$\left[k_P(T) + k_B(T)\right]/2$
$k_{top}(T)$	$\left\lfloor k_P(T) + k_{Top}(T)\right\rfloor/2$

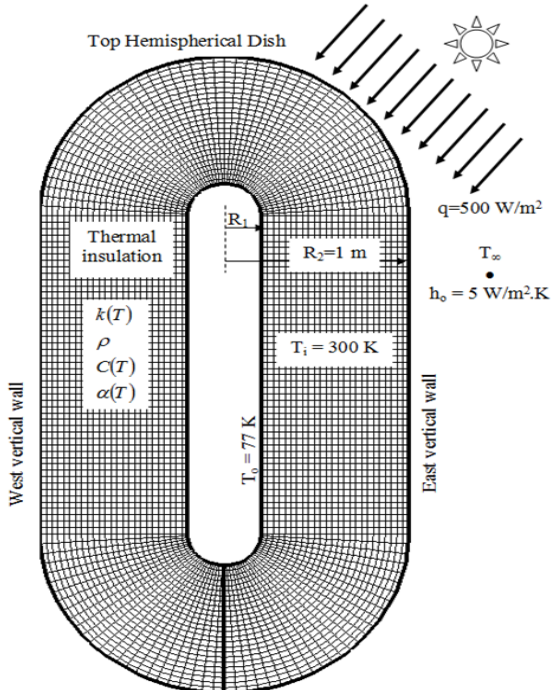

Fig. 4. Initial and boundary conditions of two-dimensional model.

(1) *Perlite in air*, $\left(R_1 = 0.2\,m, d_m = 0.5\,mm, \rho = 64\,kg/m^3\right)$.

(2) *Perlite−vacuum*, $\left(R_1 = 0.8\,m, d_m = 0.5\,mm, \rho = 50\,kg/m^3\right)$.

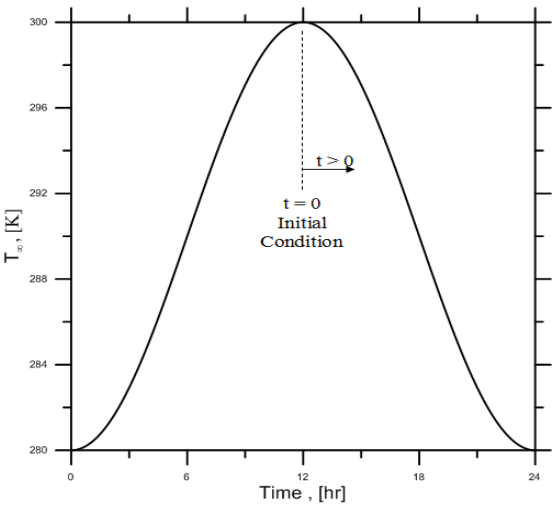

Fig. 5. Change of atmospheric temperature during a typical day.

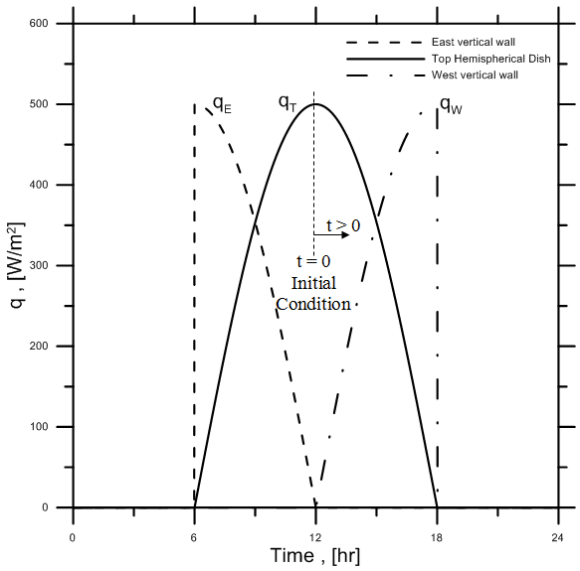

Fig. 6. Change of incident solar radiation on the wall surfaces of the storage tank in a typical day.

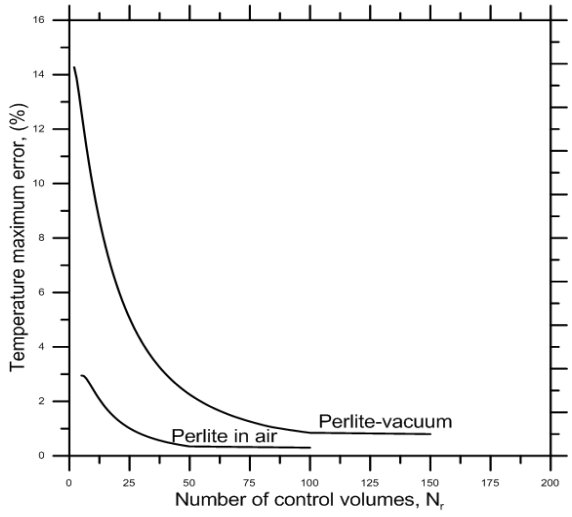

Fig. 7. GIT test of one-dimensional model.

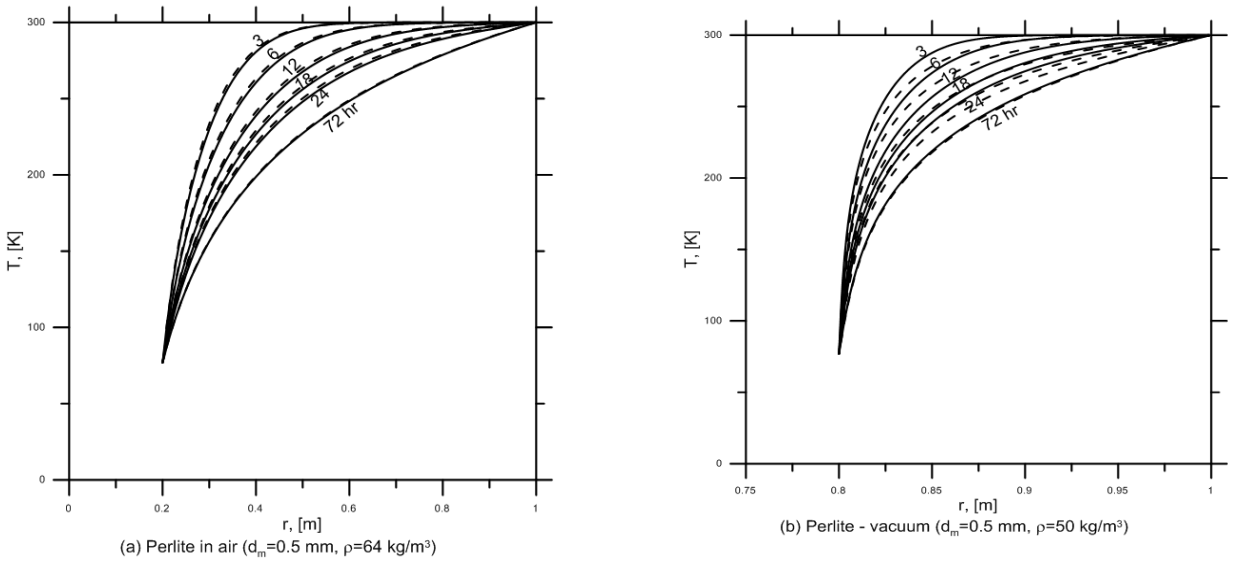

(a) Perlite in air (d_m=0.5 mm, ρ=64 kg/m³)

(b) Perlite - vacuum (d_m=0.5 mm, ρ=50 kg/m³)

(1) Temperature

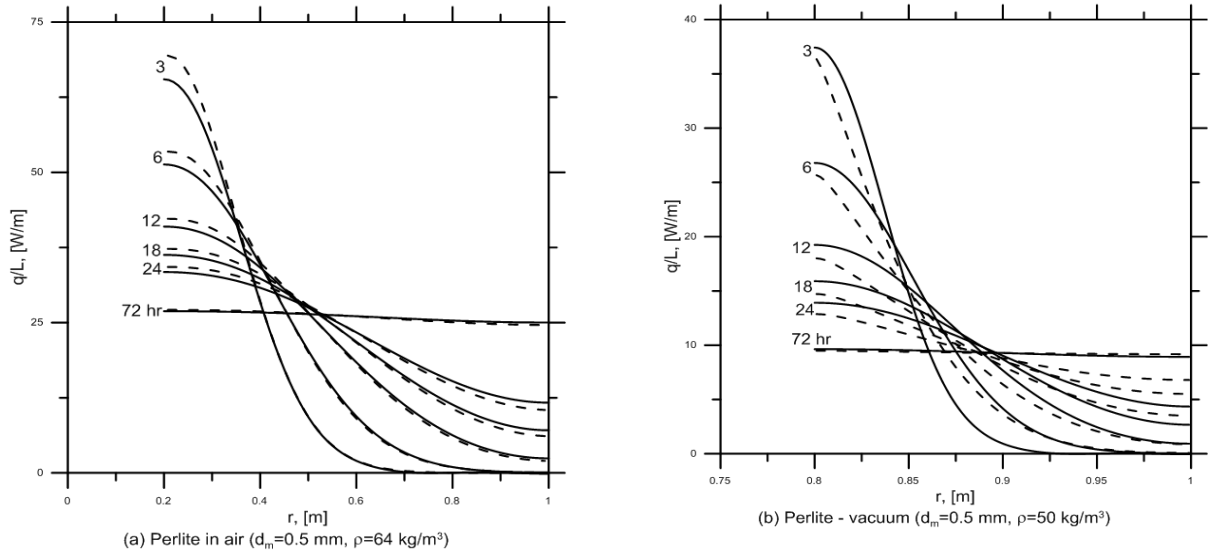

(a) Perlite in air (d_m=0.5 mm, ρ=64 kg/m³)

(b) Perlite - vacuum (d_m=0.5 mm, ρ=50 kg/m³)

(2) Heat transfer.

Fig. 8. Time history of predicted results for one-dimensional model.

(i) Solid line: Analytical solution, [5]
(ii) Dashed line: Numerical solution FVM [Present work].

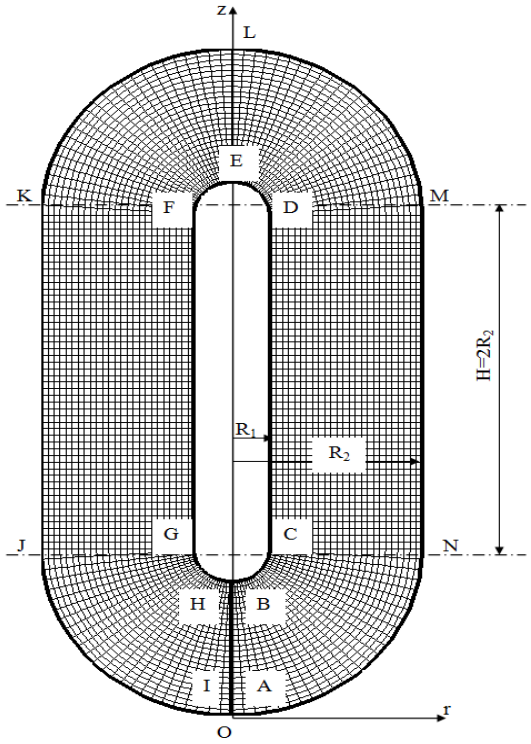

(a) Physical domain

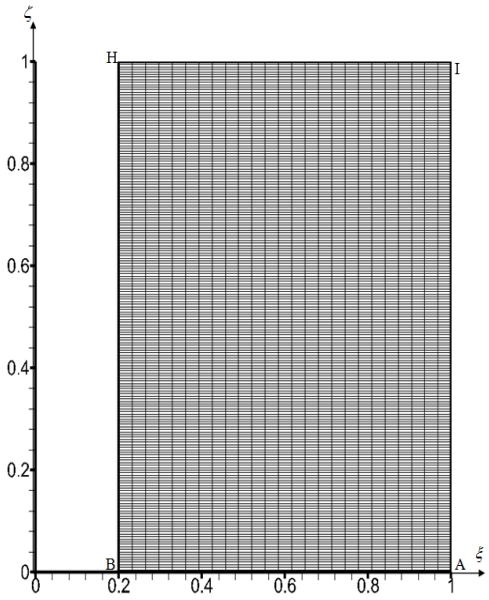

(b) Computational domain

Fig. 9. Two dimensional model, (Grid resolution =25X200).

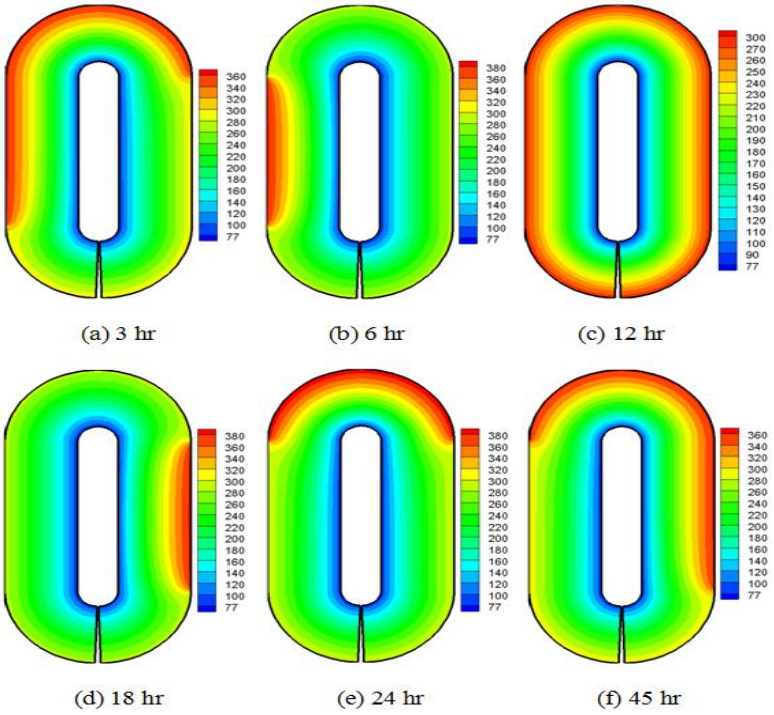

(a) Temperature, [K].

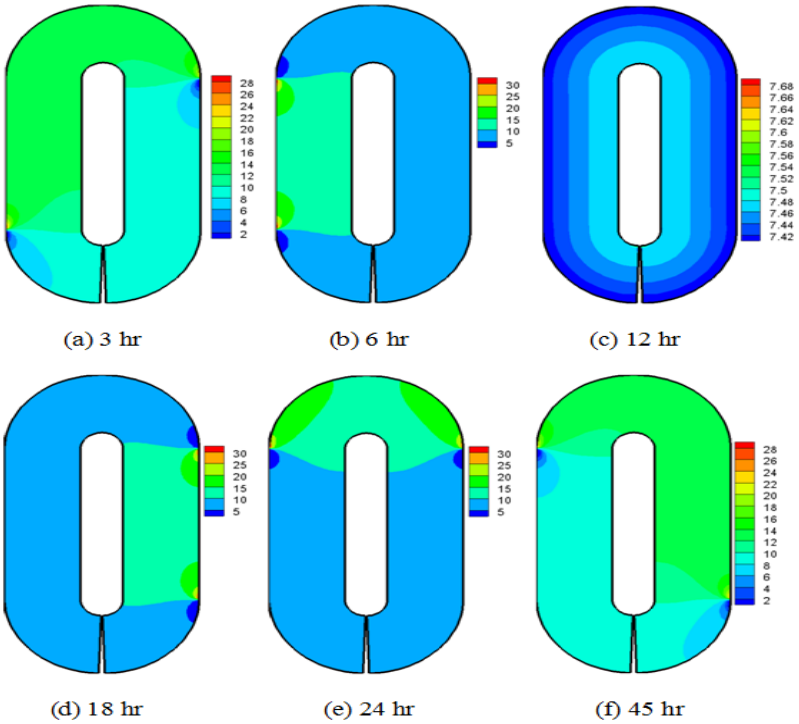

(b) heat flux, [W/m^2]

Fig. 10. Time history of predicted results for two-dimensional model, insulation material: Perlite in air (d_m=0.5 mm, ρ=64 kg/m^3).

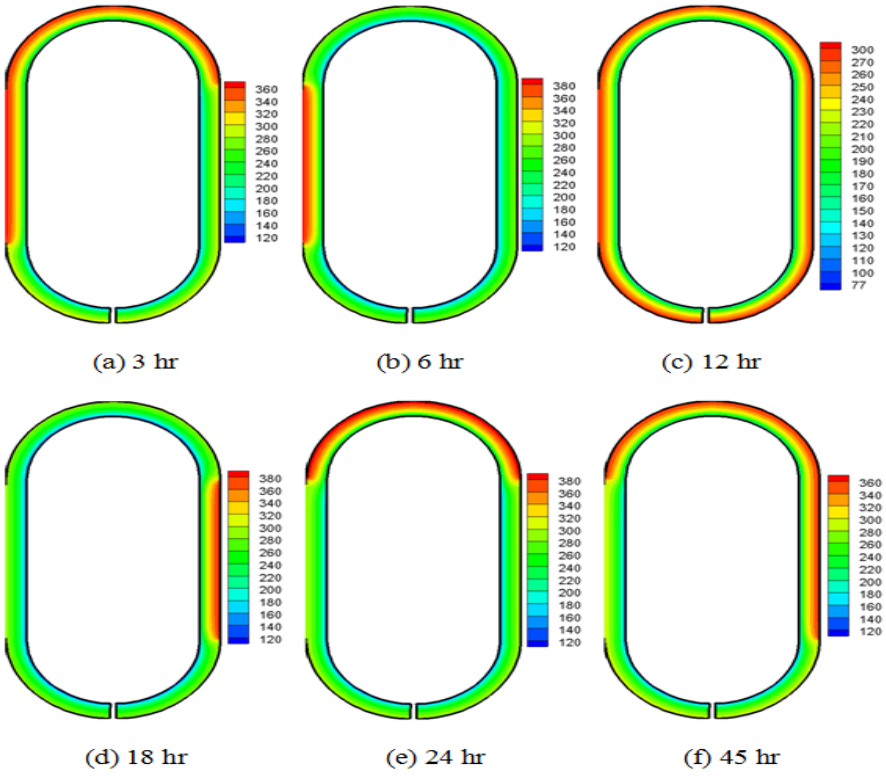

(a) Temperature, [K].

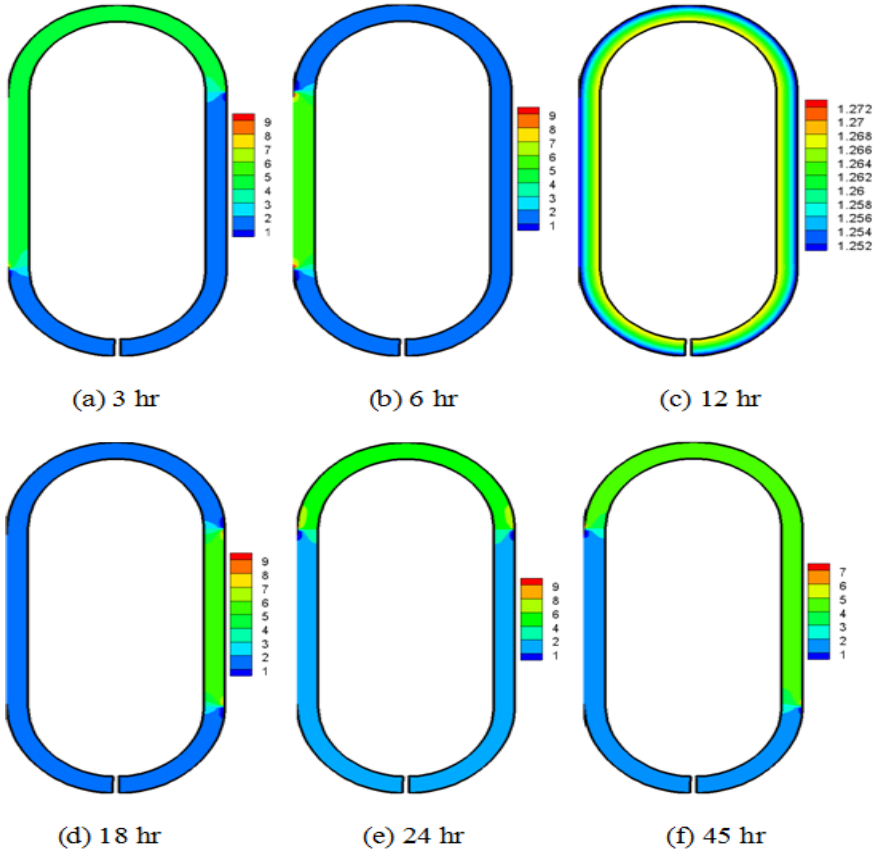

(b) heat flux, [W/m^2].

Fig. 11. Time history of predicted results for two-dimensional model, insulation material: Perlite - vacuum (d_m=0.5 mm, ρ=50 kg/m^3).

6. Conclusions

It is found that the characteristics of the thermal insulation material and the pressure value between its particles have a major effect on the rate of heat transfer and temperature profile. The dominant mode of heat transfer when choosing a specific thermal insulation material at atmospheric pressure is by heat conduction of the interstitial gas between its particles, whereas the heat transfer by radiation is negligible. When the pressure within a thermal insulation material is lowered to a vacuum level, the percentage of heat transfer by heat conduction of the interstitial gas between its particles becomes negligibly small when compared with the percentage heat transfer by radiation and conduction over the bulk material.

On the other hand, a maximum increase of about $(80\,K)$ is observed when comparing the temperature value of the thermal insulation material at the projected area of the outer surface of the Two-Dimensional model that is facing the moving source of the incident solar radiation with that of the One-Dimensional model. This increase in the temperature is due to the presence of the incident solar radiation and the natural convection heat transfer boundary condition that is associated with a periodic change in ambient temperature.

In general, the optimum selection of thermal insulating material for a specific cylindrical storage tank of liquefied cryogenic fluid is that with a minimum heat leakage (minimum boil off rate of cryogenic fluid), a minimum amount of insulating material (minimum cost) and a maximum storage capacity of the storage tank (minimum thickness of the thermal insulating material). This optimum selection is accomplished when choosing the Perlite of density $\left(\rho = 50 kg/m^3\right)$ at a gas pressure $\left(\leq 0.1 Pa\right)$ when compared with Perlite of density $\left(\rho = 64 kg/m^3\right)$ at $\left(10^5\ Pa\right)$ atmospheric pressure.

7. References

[1] Singh S., Jain P.K., Rizwan-Uddin, "Analytical solution to transient heat conduction in polar coordinates with multiple layers in radial direction", International journal of thermal sciences, ELSEVIER, 47, 261-273, 2008.

[2] Zivkovic M.M., Nikolic A.V., Slavkovic R.B. and Zivic F.T., "Non-Linear transient heat conduction analysis of insulation wall of tank for transportation of liquid Aluminum", Thermal Science, Vol. 14, Suppl., S299-S312, 2010.

[3] Jain P.K., Singh S. and Rizwan-uddin, "An exact analytical solution for two-dimensional, unsteady, multilayer heat conduction in spherical coordinates", International journal of heat and mass transfer, ELSEVIER, 53, 2133-2142, 2010.

[4] Amiri D.A., Kayhani M.H., Norouzi M., "Exact analytical solution of unsteady axi-symmetric conductive heat transfer in cylindrical orthotropic composite laminates", International journal of heat and mass transfer, ELSEVIER, 55, 4427-4436, 2012.

[5] Mishaal Abdulameer Abdulkareem, "Analytical Solution of Transient Heat Conduction through a Hollow Cylindrical Thermal Insulation Material of a Temperature Dependant Thermal Conductivity", Journal of Engineering, University of Baghdad, Volume 19, No. 11, 1483-1503, November 2013.

[6] Mishaal Abdulameer Abdulkareem, "Analytical Solution of Transient Heat Conduction through a Hollow Spherical Thermal Insulation Material of a Temperature Dependant Thermal Conductivity", Journal of Engineering, University of Baghdad, Volume 20, No. 1, 78-97, January 2014.

[7] Hofmann A., "The thermal conductivity of cryogenic insulation materials and its temperature dependence", Elsevier, Cryogenics, 46, 815-824, 2006.

[8] Veersteeg H.K. and Malalasekera W., "An Introduction to Computational Fluid Dynamics: The Finite Volume Method", Longman Scientific & Technical, England, 1995.

[9] Holman J.P., "Heat Transfer", 7th ed in SI Units, McGraw Hill, UK, 1992.

[10] Hoffmann, K.A., "Computational Fluid Dynamics for Engineers", Engineering Education System, Austin, Texas, USA, 1989.

[11] Corruccini R.J. and Gniewek J.J., "Specific Heats and Enthalpies of Technical Solids at Low Temperatures", NBS Monograph, 21, 1960.

Nomenclature

a	Constant
B, b	Bottom
b	Constant
c	Constant
C	Specific heat Capacity, kJ/kg.K
d	Particle diameter, mm
E, e	East
H	Height, m
h_o	Free convection heat transfer coefficient, $W/m^2.K$
k	Thermal conductivity, W/m.K
N	Number of control volumes
N, n	North
q	Heat flux of incident solar radiation, W/m^2
r	Distance along the r-direction, m
S, s	South
R_1	Inner radius, m
R_2	Outer radius, m
T	Temperature, K
Time	Time, hr
Top	Top
top	Top
t	Time, second
W, w	West
z	Distance along the z-direction, m

Greek symbols

Δ	Change in magnitude
ρ	Density, kg/m^3
ξ	ξ-direction
ζ	ζ–direction

Subscripts

i	Initial
m	Mean
max	Maximum value
min	Minimum value
o	Inner surface
∞	Ambient air

Superscripts

o	Old

Abbreviation

FVM	Finite Volume Method
GIT	Grid Independency Test
TDMA	Tri-Diagonal Matrix Algorithm

تحري عددي لتوصيل الحرارة المتغير مع الزمن خلال عازل للحرارة ذات خواص حرارية متغيرة مع درجة الحرارة

مشعل عبد الأمير عبد الكريم
قسم الهندسة الميكانيكية/ كلية الهندسة / الجامعة المستنصرية
البريد الالكتروني: dr.mishal04@gmail.com

الخلاصة

تم إجراء دراسة عددية لتوصيل الحرارة ثنائي البعد المتغير مع الزمن خلال عازل للحرارة ذات خواص حرارية متغيرة مع درجة الحرارة باستخدام طريقة الحجوم المحددة. تم افتراض أن هذه المادة العازلة كانت في البداية بدرجة حرارة منتظمة وثابتة . ثم تعرضت إلى تغير مفاجئ في درجة الحرارة وبقيمة ثابتة عند سطحها الداخلي وتعرضت إلى انتقال الحرارة بالحمل الحر مقترن بتغير دوري في درجة حرارة الجو وكمية الطاقة الحرارية الناتجة الإشعاع الشمسي. تم اختيار مادتين مختلفتين لعزل الحرارة. تم اختيار الانموذج الضمني التام ليمثل التجزئة الزمنية للحل العددي. تم اختيار قيمة المعدل الحسابي للتوصيل الحراري لتمثل القيمة التقريبية للتوصيل الحراري عند الحد الفاصل بين الحجوم المحددة المتجاورة كما تم استخدام معادلة من الدرجة الرابعة لتمثل قيمة السعة الحرارية النوعية للعازل والتي تعتمد على درجة الحرارة. تم الحصول على توافق جيد عند مقارنة النتائج العددية مع تلك المتحصلة من الحل الرياضي.